Comprehensive characterization of $Fe_3O_4@Ag$ nanoparticles using cross-techniques: inference of the type of $Ag - Fe_3O_4$ interaction and its impact on anion adsorption

M. D. C. García-Onsurbe $^{\rm a},$ J. L. Roca-González $^{\rm b},$ F. Gimeno $^{\rm b},$ J. Abad $^{\rm c},$ M. Caravaca $^{\rm b}$ *, A. Soto-Meca $^{\rm b}$

In this study, magnetite nanoparticles were functionalized with metallic silver using a chemical reduction method, and their structural, morphological, thermal, electrokinetic and magnetic properties were characterised using thirteen complementary techniques. Combined analysis by Transmission Electron Microscopy (TEM), Scanning Electron Microscopy (SEM), X-ray Diffraction (XRD), Fourier Transform Infrared Spectroscopy (FTIR), Raman Spectroscopy (Raman) and X-ray Photoelectron Spectroscopy (XPS) revealed a promising surface configuration, where silver is deposited on the surface of magnetite as metallic Ag⁰, forming nanoclusters without penetrating the spinel crystal lattice or altering the iron's oxidation state. This configuration generates a biphasic system, where magnetite retains its magnetic properties while silver provides a modulated surface capable of interacting electrostatically with anionic species. The synthesis and characterization approach were comprehensive, following a multi-technique strategy where each technique reinforced or limited the interpretations of others: XRD confirmed the crystalline identity, XPS ruled out chemical bonding, and Raman-FTIR complemented vibrational analysis. TEM and SEM revealed surface organization, while Brunauer-Emmett-Teller Surface Area Analysis (BET) and laser diffraction characterized porosity and dispersion. Thermogravimetry (TG)- Differential Scanning Calorimetry (DSC) studies demonstrated enhanced thermal stability and Point of Zero Charge (PZC) analysis provided evidence of electrostatic modulation, with magnetometry confirming the magnetic retention after functionalization. This integrative strategy not only validated the physical nature of the silver-magnetite interaction but also demonstrated that silver acts as an electrostatic modulator without compromising internal magnetism. The combination of Van der Waals interactions, increased surface area, and localized positive charge regions favours the adsorption of anionic pollutants. This was corroborated in previous adsorption experiments (e.g., nitrate and amoxicillin removal), confirming the material's potential in environmental decontamination applications. In conclusion, the rational design of Fe₃O₄@Ag systems through surface functionalization with silver enables the integration of physical, thermal and electrostatic enhancements, which, when analysed through a coherent multi-technique methodology, converge toward a single functional objective: the development of effective adsorbent nanomaterials for water treatment.

(Received July 7, 2025; Accepted October 6, 2025)

Keywords: magnetic nanomaterials, nanocomposites, adsorption mechanisms, water remediation, surface characterization, environmental studies

1. Introduction

The design of functionalized nanomaterials for environmental decontamination has emerged as a priority area in materials science, driven by the need for versatile, selective and efficient systems. In this context, magnetite (Fe₃O₄) has been widely used as a magnetic core due to its

^a Campus Alfonso XIII, Technical University of Cartagena, 30203 Cartagena, Spain

^bUniversity Centre of Defence at the Spanish Air Force Academy, MDE-UPCT, C/Coronel López Peña s/n, 30720, Santiago de la Ribera, Murcia, Spain ^cDepartment of Applied Physics, Technical University of Cartagena, Campus Muralla del Mar, Cartagena 30202, Spain

^{*} Corresponding author: manuel.caravaca@cud.upct.es https://doi.org/10.15251/DJNB.2025.204.1189

biocompatibility, stability and ease of recovery using magnetic fields (1–3). However, its adsorbent capacity can be improved through surface modifications that increase the specific area, modify the surface charge and generate new active sites, thus expanding its effectiveness in removing contaminants

Numerous studies have addressed the synthesis of silver-functionalized Fe₃O₄ nanoparticles, but generally with limited characterization. For example, different combinations of techniques such as XRD, SEM, TEM, FTIR or TG have been used to evaluate the crystalline structure, morphology or thermal stability of these hybrid systems (4–7).

However, most of these studies do not incorporate complementary methodologies such as XPS, PZC or laser diffraction, nor do they critically address the type of interaction between silver and the magnetite support, as proposed in recent studies (8–10). Recommendations gathered in recent reviews highlight precisely the importance of adopting cross-modal and multimodal approaches to achieve reliable inferences in complex nanocomposites (8,11).

This work aligns with this perspective, developing a systematic study of Fe₃O₄@Ag nanoparticles obtained by chemical reduction with NaBH₄, applying a battery of characterization techniques unprecedented in this context. XRD, SEM, TEM, EDX, FTIR, Raman, XPS, TG, DSC, BET, PZC and laser diffraction have been used, allowing us to construct an integrated and accurate view of the structure, morphology, surface chemistry, thermal stability and adsorbent functionality of the nanocomposite.

Among the most relevant findings is the identification of Ag⁰ clusters anchored superficially to magnetite without oxide formation or electronic interaction with Fe. This behaviour had already been suggested by electron microscopy by (4), who observed spherical clusters of fine particles agglomerating on magnetite, with primary sizes of approximately 16 nm, with no evidence of structural integration.

Likewise, our own TEM and XPS analyses confirm a heterogeneous and non-uniform surface distribution of Ag⁰, consistent with surface metal clustering. From the integrated combination of multiple techniques—including XPS, XRD, FTIR, Raman, TG, BET, and PZC—it is inferred that the interaction between silver and magnetite is predominantly physical, characterized by Van der Waals and London dispersion forces, with no evidence of chemical bonds. This conclusion is essential for understanding the mechanism by which silver reorganizes the surface of the support and enhances its adsorbent capacity.

This work also addresses a key challenge identified in recent reviews on surface characterization of nanomaterials: the need to correlate structural, morphological and surface properties with functional performance. By integrating thirteen complementary techniques, our study provides a comprehensive and synergistic approach to understanding the surface interactions and validating the adsorption efficiency of the system, in line with emerging recommendations in the field (8,11).

2. Preparation of Fe₃O₄ and Fe₃O₄@Ag nanoparticles

To ensure the comparative validity of the characterization techniques applied, two types of magnetite samples were prepared: one synthesized in the laboratory from ferric and ferrous salts $(\text{FeCl}_3 \cdot 6\text{H}_2\text{O} \text{ y FeCl}_2 \cdot 4\text{H}_2\text{O})$, and another of commercial origin with high purity $(\text{Fe}_3\text{O}_4, 99\%, \text{NanoGrafi})$, selected for its uniform morphology and well-defined crystalline structure, which allowed for better diffractometric analysis and control in techniques such as XRD, SEM and laser.

Magnetite was synthesized by coprecipitation in an alkaline medium under a nitrogen atmosphere, adding concentrated ammonia to a solution of Fe(III) and Fe(II) in a 2:1 molar ratio, maintaining agitation for 10 minutes at 80 °C. The particles obtained were separated using a neodymium magnet, repeatedly washed with distilled water until a neutral pH was achieved, and redissolved in water for subsequent functionalization. Functionalization with silver was carried out following a procedure adapted from references (12) and (9), although adjusting the molar ratios to a specific value of 0.25 between Ag and Fe₃O₄ to optimize the surface distribution of silver. To

achieve this, a solution of silver nitrate (AgNO₃, 0.0917 g) was slowly added to an aqueous suspension of 500 mg of magnetite under constant stirring. The reduction of Ag⁺ ions to Ag⁰ was carried out by the controlled addition of sodium tetraboride (NaBH₄, 0.0204 g) dissolved in water, observing a colour change characteristic of the formation of metal nanoparticles.

The mixture was stirred for at least one hour to ensure complete functionalization, after which the solid was thoroughly washed with distilled water to remove by-products and residual reagents. The functionalized $Fe_3O_4@Ag$ particles obtained were dried and stored for further characterization.

This procedure was repeated with slight variations in the Ag/Fe₃O₄ molar ratios for adsorption and control tests. In addition, the use of commercial magnetite together with the synthesized magnetite allowed the results to be validated through inter-synthetic replicability, thereby reinforcing the reliability of the data obtained by the different techniques applied.

2.1. Scanning electron microscopy, transmission electron microscopy and energy dispersive X-ray spectroscopy

The morphological and compositional characterization of the nanoparticles was performed using SEM, TEM and EDX. These complementary techniques offer insight into both the structural evolution of the material during silver functionalization and the subsequent adsorption of nitrate anions. SEM and EDX provide valuable surface-level information that supports findings from more specific spectroscopic and textural analyses (4,5,7,9). To highlight the practical role of these techniques in confirming contaminant retention, nitrate was selected as a model pollutant due to its environmental relevance in eutrophication processes affecting coastal lagoons.

SEM and EDX were carried out using a Hitachi S-4800 field emission scanning electron microscope operating at an acceleration voltage of 5.0 kV. This equipment allows high-resolution images to be obtained without the need for metal coating, which is particularly suitable for the analysis of sensitive materials. Morphological characterisation was complemented by energy dispersive X-ray spectroscopy (EDX), which provides qualitative information on elemental composition. TEM was performed using a JEOL model JEM-1400 Plus, 120 kV electron microscope equipped with a GATAN model ORIUS image acquisition camera. This system allows high-resolution images (0.38 nm between points and 0.2 nm between lines) to be obtained and is equipped with a sample holder for four grids, facilitating sequential analysis. The technique allows the morphology (shape, dimensions and distribution) of microcrystals or nanoparticles to be determined, as well as their crystalline structure and elemental composition.

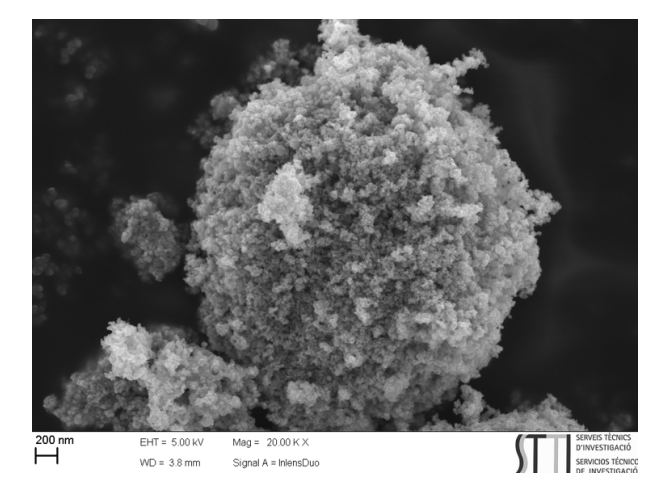


Fig. 1. SEM micrograph of pure Fe₃O₄. The image shows a compact agglomerate composed of nanosized particles with uniform surface coverage. No structural irregularities or bright contrast areas are observed, consistent with non-functionalized magnetite. The surface appears homogeneous, without evidence of metallic phases or surface modifications.

SEM images are shown in Figure 1, Figure 2 and Figure 3 corresponding respectively to pure magnetite (Fe₃O₄), silver-functionalized magnetite (Fe₃O₄@Ag), and nitrate-exposed silver-functionalized magnetite (Fe₃O₄@Ag-NO₃). Figure 1 displays quasi-spherical particles with a homogeneous distribution and smooth surfaces, characteristic of the unmodified material. No regions of high contrast or surface roughness are detected, and the overall morphology appears consistent with non-functionalized magnetite. In contrast, Figure 2, which corresponds to the silver-functionalized sample, reveals the emergence of discrete bright spots dispersed across the surface. These high-contrast points are attributed to metallic silver aggregates (Ag⁰), whose increased brightness in SEM imaging arises from their higher atomic number Z (13,14). This observation is supported by backscattered electron theory, where the signal intensity is approximately scaled with atomic number according to the empirical relationship I \propto Z^{1.7}. Although the SEM images were acquired in standard secondary electron mode, certain Ag-rich domains still exhibit a detectable contrast relative to the Fe₃O₄ matrix.

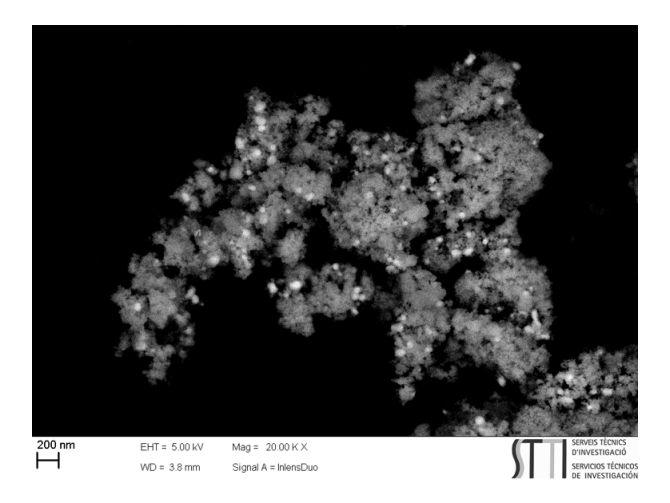


Fig. 2. SEM micrograph of silver-functionalized Fe₃O₄ (Fe₃O₄@Ag). The image reveals dispersed aggregates of nanosized particles with numerous bright contrast points across the surface, attributed to metallic silver (Ag⁰) clusters. These features are absent in the unmodified sample, suggesting successful surface functionalization. Morphological changes such as increased surface roughness and looser packing are also observed.

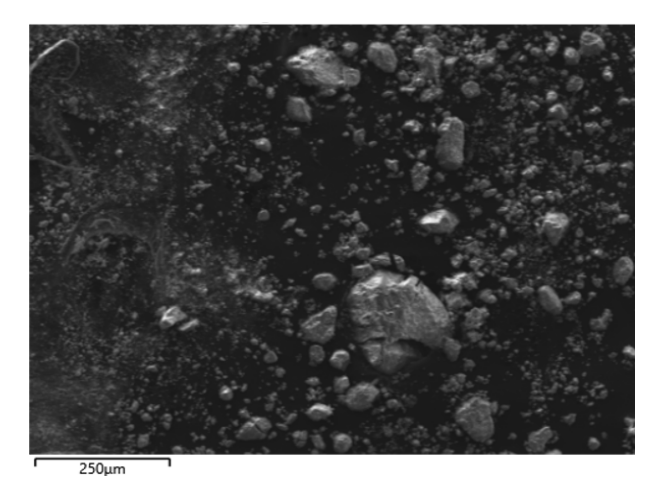


Fig. 3. SEM micrograph of Fe₃O₄@Ag after NO₃⁻ adsorption. The surface exhibits strong morphological heterogeneity, characterized by large aggregates and fine particles that are irregularly distributed. These features suggest surface restructuring associated with the adsorption of nitrate anions.

However, it is important to note that under these imaging conditions, the silver is not always distinctly resolved. In fact, the absence of clear structural contrast in some areas highlights the limitations of SEM for direct elemental discrimination, especially in secondary electron mode and at low accelerating voltages. To address this, backscattered electron (BSE) imaging is often more suitable for identifying heavier elements, such us Ag, Cu or Au, due to their enhanced signal. This limitation is evident in Figure 1, where no visual cue allows one to distinguish silver from magnetite—emphasizing the need for complementary analysis. In practice, the presence of Ag was verified by EDX spectroscopy, as discussed below.

Figure 3 corresponds to the sample exposed to nitrate. The morphology appears highly heterogeneous, with both large aggregates and fine submicrometric structures unevenly distributed across the surface. The microstructure shown is representative of the material after nitrate adsorption, reflecting surface disorder and a broad particle size distribution. EDX analysis confirmed the presence of nitrogen, supporting the hypothesis of successful nitrate retention on the functionalized surface. This phenomenon could be mediated by electrostatic interaction (weak ionic attraction), since NO₃⁻, as a negatively charged anion, tends to adhere to locally positive surfaces, such as those generated by charge redistribution around Ag⁰ nanoparticles. This hypothesis is supported by the changes observed in the zero-charge point (ZCP), both in this study and in the works of (15) and (10), where it is shown that the presence of silver shifts the ZCP towards more acidic values, favouring the attraction of anions. The areas of highest electronic contrast could reflect active microdomains where the accumulation of anions has favoured the formation of secondary aggregates, in line with the findings of (5,6,16,17) in Ag-functionalized hybrid systems (7,18).

Taken together, the SEM observations highlight progressive changes in morphology throughout the functionalization process. Nonetheless, care must be taken when interpreting these images, as SEM alone does not provide unambiguous elemental identification. For that reason, all morphological interpretations were corroborated with EDX spectra and elemental mappings, which confirm the presence of Fe, O, and Ag in the functionalized samples, as well as traces of N in nitrate-treated ones. These complementary results are essential to understand the surface organization and interaction dynamics at the nanoscale.

TEM images confirm these patterns: in pure magnetite (Figure 4), the quasi-spherical nuclei appear well defined, with sharp edges and homogeneous morphology (19). No amorphous halos or signs of external coating are observed, confirming the absence of functionalizing elements. The high contrast of the core is characteristic of pure magnetite, with regular distribution and no significant aggregation; in contrast, in the silver-functionalized sample (Figure 5), heterogeneous dark halos surrounding the cores are detected, which can be interpreted as amorphous metal clusters or superficially distributed Ag⁰ deposits. This non-uniform distribution and the absence of integration into the spinel network reinforce the hypothesis that silver is anchored by weak physical interactions—such as Van der Waals forces or London dispersion—without forming covalent bonds or metal oxides. The observed morphology is consistent with the metallic clustering described by authors such as (7) and (4), who also documented discontinuous surface structures in Agfunctionalized nanocomposites using high-resolution TEM (8,20).

One of the strengths of TEM is precisely its ability to reveal the presence of amorphous surface coatings on functionalised nanoparticles. In previous work, both in nanoparticles treated with L-cysteine and in those exposed to contaminants such as amoxicillin, the appearance of a diffuse veil around the magnetic cores has been documented by TEM. In the first case, this veil is attributed to the organic coverage generated by functionalisation with L-cysteine, while in the second case it is interpreted as direct evidence of surface interaction between the contaminant and the nanoparticle (7,21). This ability of TEM to detect microstructures associated with adsorption or functionalisation phenomena makes it a powerful tool for studying non-crystalline coatings that cannot be resolved by other conventional techniques.

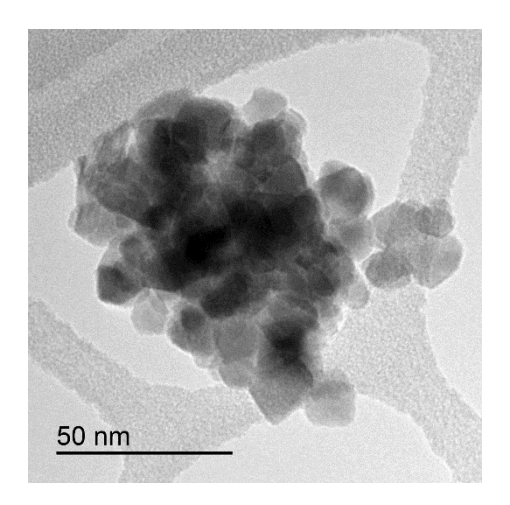


Fig. 4. TEM of pure magnetite (Fe₃O₄, Nanografi). Well-defined quasi-spherical cores with no visible coating. No amorphous halos or additional structures are observed, confirming the absence of functionalization.

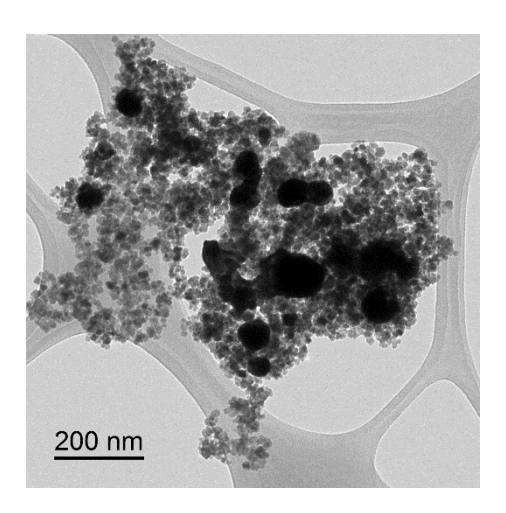


Fig. 5. TEM of silver-functionalized magnetite ($Fe_3O_4@Ag$). Dark halos are observed around the nuclei, consistent with surface metal clusters of Ag^0 . The uneven distribution and contrast suggest adsorption without structural integration.

To evaluate the adsorption of nitrate anions onto the silver-functionalized magnetite, EDX analysis was performed on the Fe₃O₄@Ag sample previously treated with a nitrate solution (Figure 6). The spectrum confirms the presence of Fe, O, and Ag as major elements. In some areas, there is a weak signal for nitrogen, which could be attributed to the surface adsorption of nitrate anions. Elemental mapping (Figure 7) reinforces this hypothesis by showing the coexistence of iron and silver with non-uniform distribution and Ag-enriched zones that could act as active adsorption centres. These distributions are consistent with those obtained in our previous work on the adsorption of amoxicillin and nitrate (7,10).

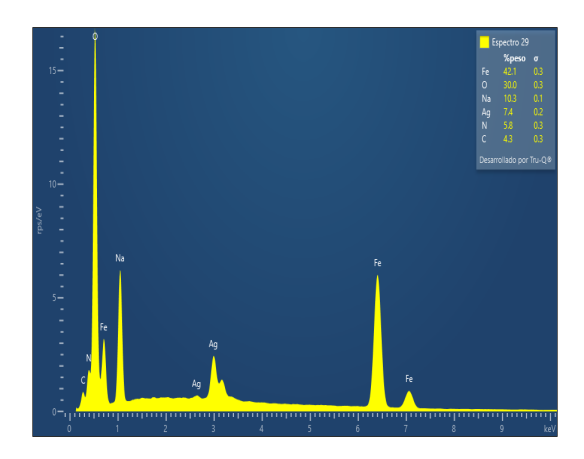


Fig. 6. EDX spectrum of Ag-functionalized Fe_3O_4 . The spectrum confirms the presence of Ag on the surface of the magnetite, together with the elements Fe and O, validating the functionalization without structural integration.

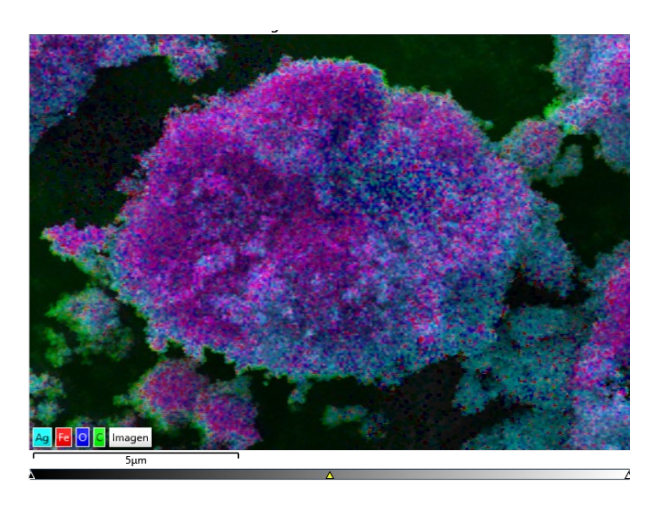


Fig. 7. EDX elemental mapping of Ag-functionalized Fe₃O₄. The mapping shows a non-uniform distribution of Ag on the oxide surface, with locally enriched areas, suggesting surface clustering without integration into the crystal lattice.

In terms of composition, EDX analyses show that in pure magnetite, the atomic percentages remain around 67-72% Fe and 26-30% O, with no signs of silver or nitrogen. In the functionalized samples, an average Ag content of between 4% and 10% is detected, while in the nitrate-treated samples, the nitrogen proportion ranges from 0.5% to 2%, suggesting partial adsorption on the surface (5-7).

From a functional point of view, these observations support a predominantly surface interaction between Fe₃O₄ and Ag, of a physical nature (Van der Waals forces, electrostatic bonding or metal clustering), rather than deep chemical integration (16). No complex intermetallic structures or notable modifications in the magnetite core were observed. These characteristics suggest that silver acts as an active but superficial metallic coating, in line with what has been described in other hybrid platforms for decontamination (7,9,22).

The advantage of EDX lies in its ability to detect and quantify multiple elements simultaneously with spatial correlation. However, its limitations include low sensitivity for light elements (such as nitrogen), potential signal interference from the sample holder or substrate (e.g., Cu), and ambiguity in distinguishing surface vs. bulk contributions. For these reasons, EDX must be interpreted cautiously and in combination with SEM and TEM to derive meaningful conclusions.

SEM reveals surface-level morphology and qualitative indicators of functionalization; TEM confirms the presence of surface clusters and structural preservation of the core; EDX validates the

presence of Ag and detects NO_3^- adsorption. Each technique has strengths and limitations: SEM offers topographical information but limited elemental contrast; TEM provides nanometric resolution and internal detail but is sensitive to beam effects; EDX yields compositional data but lacks depth resolution and sensitivity to light elements. Their combined application supports the hypothesis that silver functionalization occurs via surface aggregation and that nitrate adsorption occurs on Ag-enriched domains, likely through electrostatic interaction. In conclusion, SEM, TEM, and EDX collectively provide a coherent characterization of the structural and elemental evolution of the Fe₃O₄@Ag system, allowing a first integrated image of its functional behaviour to be constructed and supporting the hypothesis of active surface interactions (5,6,17). These findings will be further correlated with spectroscopic and surface techniques in subsequent sections.

2.2. Fourier-transform infrared spectroscopy

FTIR is a non-destructive vibrational technique that allows functional groups to be characterized and chemical interactions on the surface of materials to be identified (8,11). In this study, the analysis focused on three types of solid samples: (i) pure magnetite (Fe₃O₄) purchased from Nanografi, (ii) silver-functionalized Fe₃O₄ (Fe₃O₄@Ag), and (iii) silver-functionalized Fe₃O₄ after exposure to a nitrate solution (Fe₃O₄@Ag + NO₃⁻). FTIR was carried out using a Thermo Nicolet 5700 spectrophotometer (Thermo Scientific), based on a continuous scanning Michelson interferometer with 45° geometry. The system achieves a spectral resolution better than 0.5 cm⁻¹ and uses a Ge/KBr beam splitter together with a DTGS/KBr detector. The equipment covers a spectral range between 12500 and 350 cm⁻¹, with a ceramic source operating at 1525 K. It has a purge gas generator to minimise environmental interference. The Smart Orbit accessory for attenuated total reflection (ATR) was used, which allows solid samples to be analysed without prior preparation. The data acquisition and processing software was OMNIC (Thermo Scientific).

The spectra corresponding to these three samples are shown in Figure 8 and Figure 9, and the comparative analysis presented below is based on them.

The spectrum of unfunctionalized magnetite shows an intense, well-defined band centred between 580–630 cm⁻¹, attributable to the T_{1u} vibrational mode of the Fe-O bond, characteristic of the spinel lattice. The absence of other relevant bands indicates high structural purity, with no –OH groups or surface contaminants. This T_{1u} mode represents a collective vibration of the Fe-O bond active in the infrared, according to predictions of group theory applied to systems with inverse spinel symmetry (5,16).

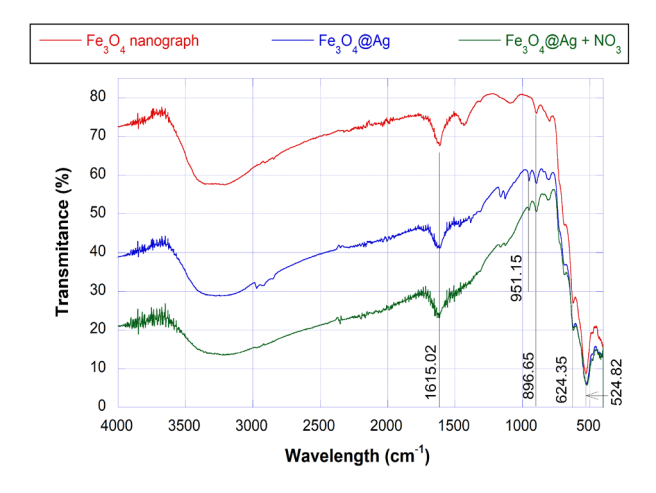


Fig. 8. FTIR spectra of Fe_3O_4 (Nanografi), Fe_3O_4 @Ag, and Fe_3O_4 @Ag after NO_3^- adsorption. All samples show the Fe_-O band at 580_-630 cm⁻¹. Only the nitrate-treated sample exhibits new bands at 1380 and 1600 cm⁻¹ (v_3 and v_1 of NO_3^-) and at 800 cm⁻¹ (v_4), confirming nitrate adsorption. The commercial Fe_3O_4 shows no additional bands, indicating high purity.

In the spectrum of silver-functionalized Fe₃O₄, the Fe-O band is preserved but shifts slightly towards lower frequencies, accompanied by a slight decrease in intensity. This effect suggests a surface disturbance of the crystal lattice induced by the presence of Ag⁰ metal nanoparticles, without the formation of new vibrational modes. In addition, a faint signal is detected around 1100 cm⁻¹, probably attributable to residual hydroxyl groups generated during the functionalization process in an aqueous medium with NaBH₄, rather than to Ag-O interactions (7,18). This assignment is expected to be confirmed by XPS analyses, where no shifts or broadening are anticipated in the Ag 3d and O 1s spectra, supporting the absence of Ag-O bonds and the stability of the surface oxygen environment. Taken together, the FTIR results reflect limited vibrational modification, consistent with the surface incorporation of metallic silver, without profound structural alteration, in agreement with the reports by (12) and (10).

The sample exposed to nitrate (Fe₃O₄@Ag + NO₃⁻) shows new spectral bands around 1380 cm⁻¹ and 1600 cm⁻¹, corresponding to the antisymmetric (ν_3) and symmetric (ν_1) stretching modes of the nitrate anion (NO₃⁻), as well as a signal at 800 cm⁻¹, attributed to the ν_4 bending mode. These signals indicate effective adsorption of the anion on the surface of the nanocomposite, which will also be supported by XPS results, as discussed later in Section 3.5, particularly by the appearance of the N 1s peak near 407.2 eV. The values observed are consistent with our article (10) and other bibliographic sources such as (16,23).

Furthermore, these vibrational changes observed by FTIR (10) are consistent with preliminary results obtained by other characterization techniques. Thermal analyses (TG–DSC) indicate greater stability after functionalization (17); BET data suggest an increase in specific surface area (18); and Raman spectra reveal signs of loss of surface order, without the formation of new phases such as hematite (18). Although these results will be discussed in detail in their respective sections, taken together, they reinforce the hypothesis that silver acts as a surface structural modifier, favouring the adsorption of contaminants through physical interactions.

In conclusion, FTIR provides valuable information on the vibrational behaviour of surface species, confirming the presence of nitrate and preserving the core structure of magnetite. Its main strength lies in the identification of functional groups, although it lacks spatial resolution and elemental specificity. When combined with techniques such as SEM, TEM and EDX, FTIR enhances a comprehensive understanding of surface interactions, which will be further developed in the Raman and XPS sections.

2.3. Raman spectroscopy

Raman spectroscopy was used to identify the crystalline phases present in the samples and detect possible structural changes after surface functionalization with silver. The analysis was performed using a LabRAM HR-800 dispersive spectrometer (Horiba Jobin-Yvon) coupled to an Olympus BX41 confocal microscope, with excitation laser lines of 514, 633 and 785 nm. The system incorporates a Peltier-cooled CCD detector and allows spectra to be obtained with a resolution of 1 cm⁻¹ in a range from 60 to 8000 cm⁻¹. A near-infrared laser line (1064 nm) is also used to minimise fluorescence in sensitive samples. The technique allows the identification of vibrational modes of specific chemical bonds and the creation of in-depth profiles or spectral mapping in functionalised materials. Its high sensitivity and versatility make it particularly useful in structural analysis at the molecular level.

Figure 10 shows the normalised Raman spectra corresponding to the pure magnetite (Fe_3O_4) and silver-functionalized magnetite $(Fe_3O_4@Ag)$ samples, respectively. The results show notable differences between the two, indicating a significant effect of the presence of Ag on the vibrational response of the system.

In the spectrum corresponding to the unfunctionalized Fe_3O_4 sample, intense peaks are observed around 227, 291 and 402 cm⁻¹, as well as a broad band centred approximately between 610 and 660 cm⁻¹, characteristic signals commonly associated with the hematite phase (α -Fe₂O₃). This observation suggests the possible coexistence of different phases of iron oxides in the sample, despite the synthesis procedure being aimed at obtaining magnetite.

However, in the silver-functionalized sample (Fe₃O₄@Ag), these signals disappear completely from the spectrum, being replaced by a more defined envelope with a dominant peak

around 670 cm⁻¹, attributable to the A₁g vibration of Fe–O in magnetite. This change suggests that the presence of silver significantly modifies the vibrational response of the material, either through a surface optical effect (shielding or modification of the local field) or by a possible partial phase transformation, which could reduce or eliminate the surface proportion of hematite initially present (22).

These results suggest that silver remains in a metallic state (Ag⁰) and is preferentially located on the surface. This interpretation will be further supported by XPS analysis, in which no signals corresponding to silver oxides are expected. Additional confirmation will be provided by TEM images and EDX mapping, showing Ag distribution at the surface. FTIR analysis shows that the characteristic vibrations of Fe-O do not undergo significant shifts, suggesting that the internal structure of the oxide remains stable and that the variations detected by Raman are mainly due to surface phenomena.

In conclusion, Raman spectroscopy offers high sensitivity to phase composition and structural variations induced by surface modification. It enables the detection of subtle vibrational differences between magnetite and hematite and helps confirm the selective presence of magnetite after silver functionalization. Its main limitation lies in its shallow penetration depth and susceptibility to fluorescence in some materials. When used alongside FTIR, SEM, TEM and EDX, Raman spectroscopy enhances the understanding of functionalization effects at the surface level and will be complemented by future XPS analysis to confirm the oxidation state of silver and possible surface interactions.

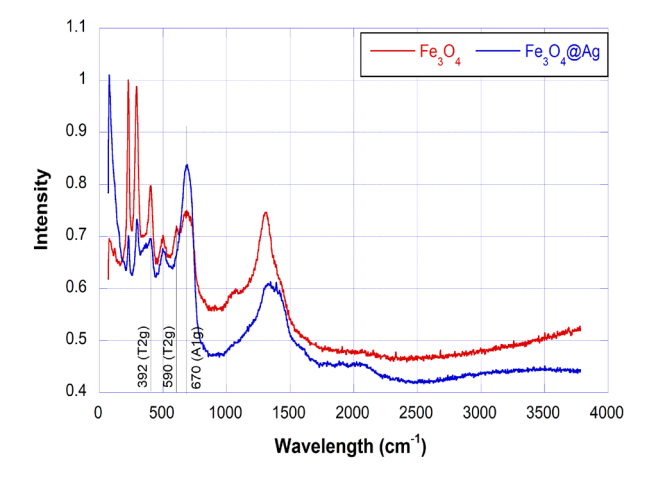


Fig. 9. Raman spectra of Fe_3O_4 and Fe_3O_4 @Ag. The pure magnetite shows bands at 227, 291, and 402 cm⁻¹, and a broad signal at 610–660 cm⁻¹, indicating partial hematite content. In contrast, the silver-unctionalized sample exhibits a dominant A_1g peak at ~670 cm⁻¹, with hematite signals absent, suggesting surface modification by Ag.

2.4. X-ray photoelectron spectroscopy

XPS enables the study of surface composition, as the attenuation length of the emitted photoelectrons is typically a few monolayers (about 1-10 nm)(24). In addition, it resolves the chemical state of the elements present in materials (8,11). X-ray photoelectron spectroscopy has been performed using a SPECS FlexPS-E spectrometer equipped with an Al Kα monochromatic source (hv = 1486.6 eV) and a PHOIBOS 150 2D-CCD hemispherical analyser. The system allows the acquisition of spectra with an energy resolution of 0.5 eV and is equipped with an ultra-high vacuum (UHV) chamber with a base pressure of less than 1×10^{-9} mbar. In this work, four types of samples were analyzed: (I) Fe₃O₄ (II) silver polycrystalline reference sample (III) Fe₃O₄ functionalized with silver (Fe₃O₄@Ag), and (IV) Fe₃O₄@Ag exposed to nitrate (Fe₃O₄@Ag + NO₃⁻).

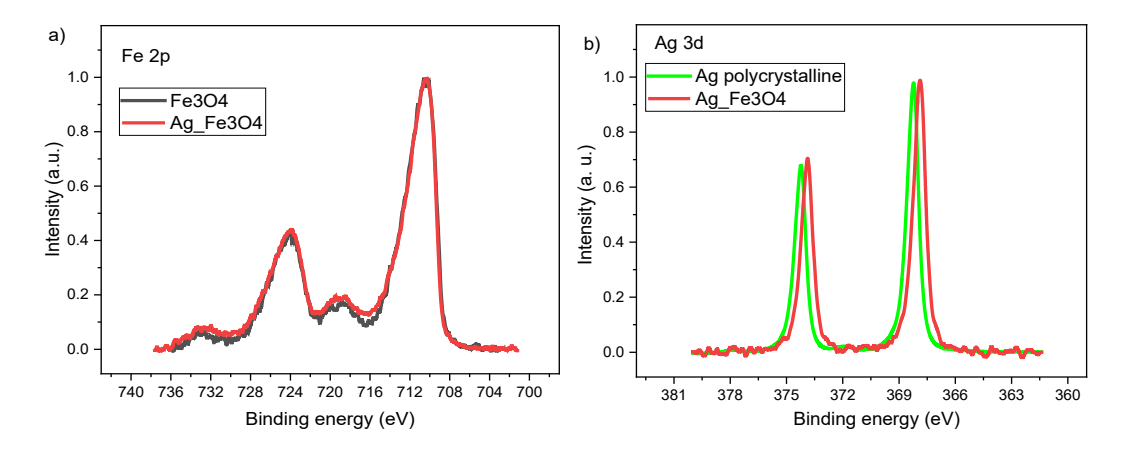


Fig. 10. XPS spectrum of a) Fe 2p for the supported magnetite (black line) and Ag NP (red line) and b) Ag 3d for an Ag polycrystalline reference sample (green line) and Ag NP supported on magnetite (red line).

Figure 10b) shows the Ag 3d core level for the Ag NP supported on magnetite (red line) and for an Ag reference polycrystalline sample (green line). The Ag 3d₅/₂ peak appears centered at 367.9 eV for the Ag NP, while for the Ag reference sample, this peak is centred at 368.2 eV, characteristic of metallic Ag (Ag⁰). The spin-orbit splitting in both samples is 6.0 eV. The 0.3 eV binding energy (BE) shift between the metallic reference sample and the Ag NP is in very good agreement with the values reported in the literature for metallic Ag NP (Ag⁰) (25) in a clear indication that the nanoparticles are metallic. Figure 10a) shows the Fe 2p core level for the pristine magnetite and the magnetite with Ag NP. Figure 10 a) shows the Fe 2p core level for the Ag NP supported on magnetite (red line) and for pristine magnetite (black line). It is interesting to note that the lineshape of both spectra is practically the same, a clear indication that there is no chemical interaction between the magnetite support and the metallic Ag NP. The Fe $2p_{3/2}$ core level is located at 710.4 eV of BE with a spin-orbit splitting of 3.6 eV. The BE of the Fe 2p is in good agreement with the values reported in the literature for magnetite (26,27). The fact of the weak interaction of the Ag NP with the magnetite and the metallic character of the NP is also confirmed by the O 1s core level shown in Figure 11 where the lineshape of this peak is almost identical. Both samples exhibit a single asymmetric peak at 529.9 eV due to the lattice oxygen of the magnetite and with a shoulder on the high-energy side at approximately 532.2 eV, which is attributed OH surface groups (28).

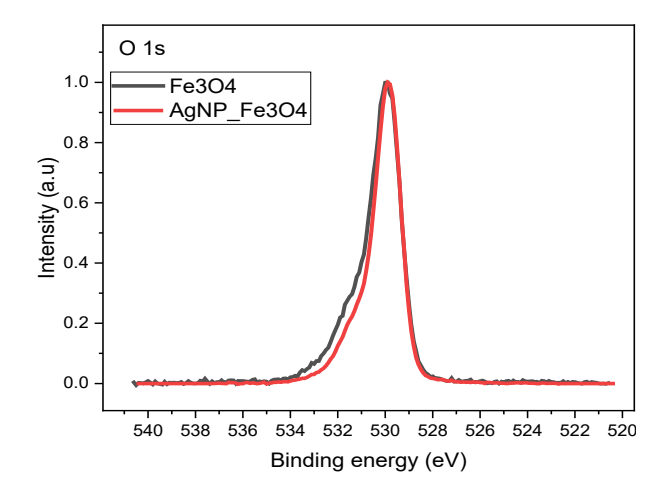


Fig. 11. XPS spectrum of O 1s for the supported magnetite (black line) and Ag NP (red line).

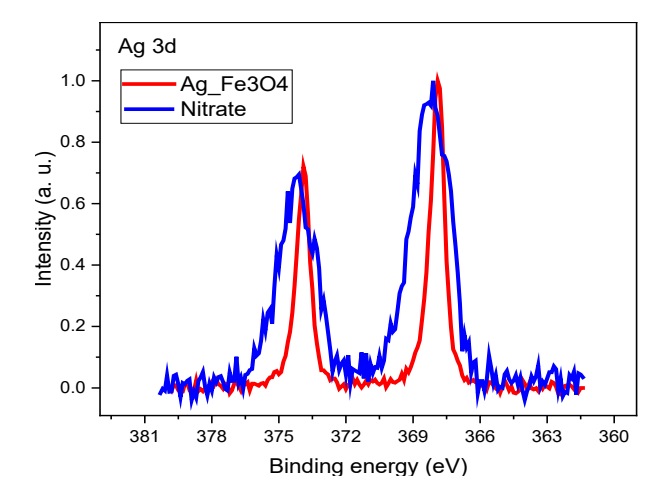


Fig. 12. XPS spectrum of Ag 3d for Ag NP supported on magnetite before (red line) and after (blue line) the nitrate adsorption.

As an example of the activity of the Ag NP, it has been studied the adsorption of nitrate on the Ag NP supported on magnetite sample. Figure 12 shows Ag 3d core level for Ag NP supported on magnetite before (red line) and after (blue line) the nitrate adsorption. It is clearly evident that new oxidation states appear in the Ag NP after the interaction with NO_3^- . Additional signals are detected around 368.2 eV and 367.4 eV, indicating the presence of surface oxides (5,20,23,29). Confirming the surface interaction between the NO_3^- anion and metallic silver (10,18). This result is consistent with previous studies reporting the successful reduction of Ag^+ ions using borohydride (7,23). Besides, the magnetite support seems to also play a role in the nitrite interaction, as is shown by the Fe 2p core level (Figure 13), where significant changes are observed after the adsorption. These facts are also confirmed by the O 1s core level (Figure 14). A shoulder appears on the low BE side, corresponding with the oxidation of Ag and Fe. On the high BE side of the spectrum, the component due to the OH surface groups increase considerably, and a new component appears assigned to H_2O (30), originating from the water present in the nitrate solution. Additionally, N is detected on the surface after the nitrate adsorption, as shown in Figure 15, where the N 1s peak appears at approximately 407.2 eV, assigned to NO_3^- (26).

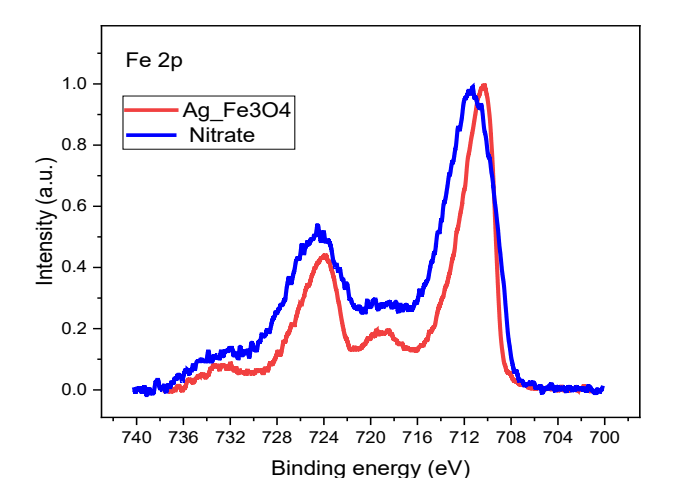


Fig. 13. XPS spectra of Fe 2p core level for Ag NP supported on magnetite before (red line) and after (blue line) the nitrate adsorption.

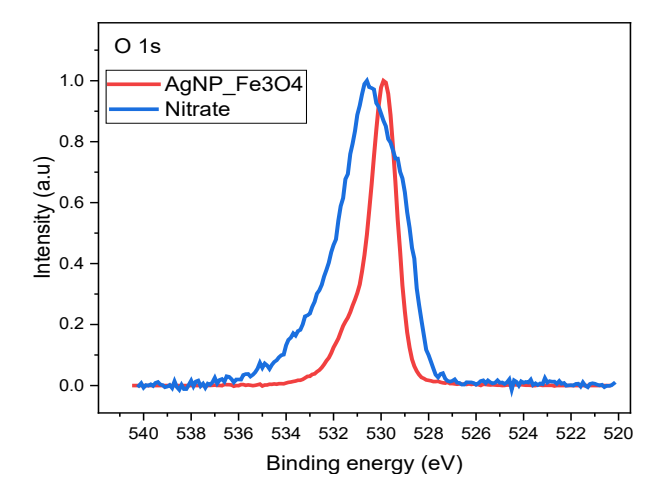


Fig. 14. XPS spectrum of O 1s for Ag NP supported on magnetite before (red line) and after (blue line) the nitrate adsorption.

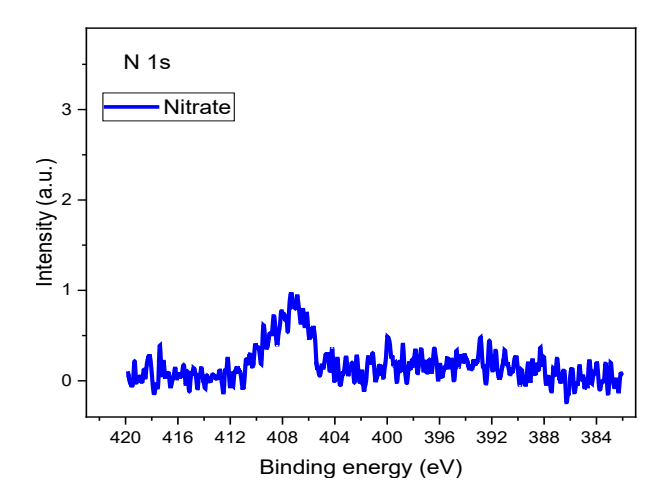


Fig. 15. XPS spectrum of N 1s for Ag NP supported on magnetite after the nitrate adsorption.

The overall interpretation of these data, reinforced by Raman structural information, suggests an interaction between Ag NP and the magnetite support with nitrate anions. Therefore, the Fe_3O_4 @Ag nanocomposite acts as a versatile and efficient platform for the adsorption of anionic contaminants, confirming its potential as a functional material in environmental decontamination processes (7,17,31). According to the XPS results, the deposited silver remains in a metallic state (Ag^0), with no evidence of oxidation or oxide formation (Ag_2O , AgO). Although this technique does not allow us to infer directly whether the silver forms metallic clusters, the low surface content (\sim 1%) and the absence of significant shifts in the Ag 3d spectrum support the hypothesis of a non-uniform distribution. This interpretation reinforces what has already been observed in the TEM images, where localized clusters compatible with the formation of silver nanoclusters on the magnetite surface are evident (4,7,23).

2.5. Thermogravimetric analysis

TG allows the study of the variation in mass of a material with respect to temperature, revealing processes such as desorption, oxidation, phase transformation or elimination of surface functional groups (5,11). In this work, the thermal behaviour of pure magnetite (Fe₃O₄) was compared with that of silver-functionalized magnetite (Fe₃O₄@Ag), obtained by chemical reduction from silver nitrate (AgNO₃) and sodium borohydride (NaBH₄). Thermogravimetric analysis is performed using a Mettler-Toledo TGA/DSC 1HT system, designed to record the loss of mass of a sample as a function of temperature or time. The equipment has a horizontal furnace that operates

from room temperature to 1600 °C, with a thermal accuracy of ± 0.5 °C and a reproducibility of ± 0.3 °C. It allows simultaneous recording of heat flow, with a resolution of 0.1 µg. It has an automatic sampler with 34 positions, automatic control of purge gases up to 200 mL/min, and can be coupled to detectors for the analysis of released gases, such as an FTIR spectrophotometer or a mass spectrometer.

Figure 16 shows the thermogravimetric (TG) curve of the pure magnetite sample (Fe₃O₄). Unfunctionalized magnetite exhibits an initial loss of mass at low temperatures, attributed to the desorption of surface water and hydroxyl groups (-OH). Subsequently, between 150 °C and 350 °C, a sharp drop in mass is observed, consistent with internal redox processes, such as the partial oxidation of Fe²⁺ to Fe³⁺, which is common in systems that are not completely thermally stabilized (5,23).

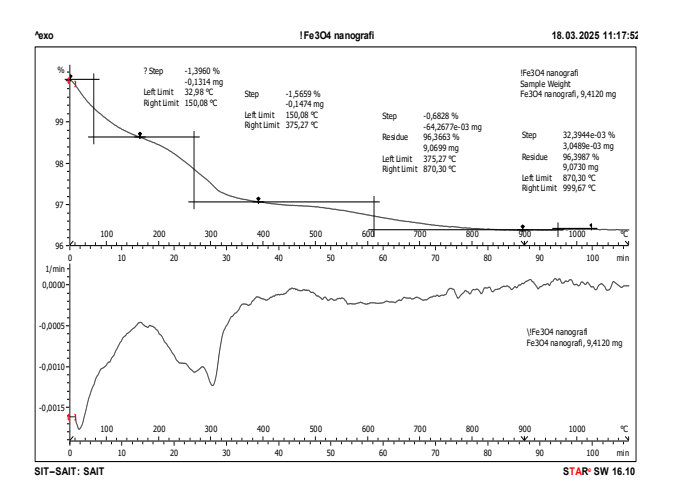


Fig. 16. The thermogravimetric curve of the pure magnetite sample (Fe_3O_4). A loss of mass is observed in two stages: an initial stage at low temperatures attributed to the desorption of water and -OH groups, and a second, more pronounced stage between $150-350^{\circ}C$, related to internal redox processes such as the partial oxidation of Fe^{2+} to Fe^{3+} .

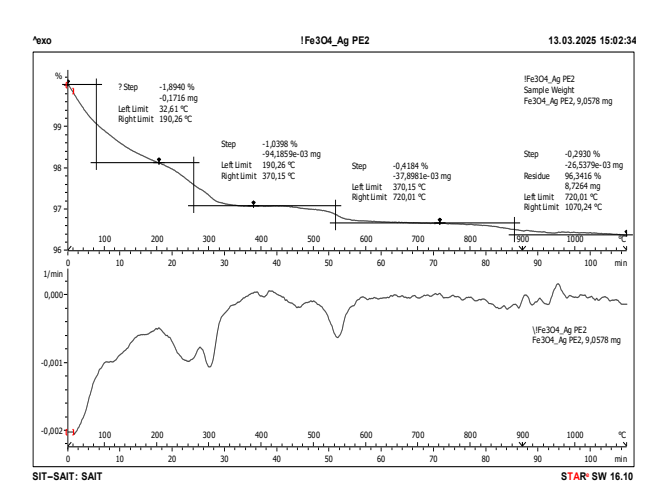


Fig. 17. Thermogravimetric curve of the silver-functionalized magnetite sample (Fe₃O₄@Ag). The mass loss is smoother and more progressive, with a less pronounced slope throughout the thermal range, indicating greater thermal stability. This behaviour suggests a surface passivation effect induced by silver, as well as a possible barrier effect against heat transfer.

In contrast, Figure 17 shows the thermogravimetric (TG) curve of the silver-functionalized magnetite sample (Fe₃O₄@Ag), which displays a more stable profile and a gradual mass loss across the entire temperature range studied. The less pronounced slope and more linear shape of the curve

indicate greater thermal stability. This effect is attributed to two main phenomena: (i) silver-induced surface passivation, which reduces the number of volatile groups (water and -OH) available for desorption; and (ii) a physical 'thermal barrier' effect, in which Ag nanoparticles act by dispersing local heat transfer at the magnetite surface (18,22).

This improved behaviour demonstrates how surface functionalization can directly influence thermal reactivity, even without altering the internal crystal structure. In this context, TG provides macroscopic evidence of the stabilizing role of Ag in the surface engineering of magnetic nanoparticles. Table 1 shows a summary of all the thermal properties analysed.

Sample	Total loss (%)	Main loss range	Relative slope	Key observations
		(°C)		
Fe ₃ O ₄	~5.6 %	150 - 350	High	Oxidation $Fe^{2+} \rightarrow Fe^{3+}$,
				loss of OH and H ₂ O
Fe ₃ O ₄ @Ag	~3.1 %	100 - 350	Low	Thermal barrier effect,
				greater stability

Table 1. Table summarising thermal properties (TG).

No abrupt losses of mass attributable to nitrate decomposition were detected, confirming that the washing process was effective and that no AgNO₃ residues remained (10). These results are consistent with XPS analyses, which show silver exclusively in its metallic state (Ag⁰), and with FTIR, which shows no significant signs of residual nitrate. Furthermore, the thermal behaviour observed is consistent with Raman and XRD analyses, which indicate that functionalization (17,18) with silver does not alter the internal crystalline phase, but significantly modifies the surface of the material.

These cross-confirmations results reinforce the value of TG as a diagnostic technique for evaluating both surface purity and structural integrity in functionalized nanomaterials. However, it must be noted that TG does not provide spatial or elemental resolution, and any thermal event must be interpreted with caution and supported by complementary techniques. Additionally, the contribution of the sample holder or crucible material at high temperatures must be accounted for, especially in small-scale tests.

Overall, the thermogravimetric results demonstrate that silver functionalization enhances the thermal resistance of magnetite without compromising its structure, which may be particularly useful in applications requiring stability against thermal variations or reactive conditions (5,22,32). This technique is especially valuable when screening nanocomposites for environmental or industrial uses where thermal cycling, surface stability and phase retention are critical.

2.6. Differential scanning calorimetry

DSC allows the analysis of thermal changes in a material as a function of temperature, detecting endothermic or exothermic transitions associated with surface reorganization processes, oxidation, loss of structural water, or phase changes (5,11). In this work, the thermal profiles of pure magnetite (Fe₃O₄) and silver-functionalized magnetite (Fe₃O₄@Ag) were compared in order to determine how functionalization affects the thermal response of the system (5,6). DSC is performed using a Mettler-Toledo DSC 822e device, which allows high-sensitivity measurement of heat flow variations between a sample and a reference. The system operates in a temperature range of -150 °C to 700 °C, with a thermal accuracy of ± 0.2 °C and a reproducibility of less than 0.1 °C. It has an automatic sampler with 34 positions, a purge gas controller and a modulated temperature option. The heating rate is programmable between 0 and 200 °C/min, and the thermal signal resolution reaches 0.04 μ W, with a response time of less than 2.3 seconds.

In the Fe₃O₄ sample (Figure 18), two main thermal events were detected: a slight endothermic signal at ~121°C, attributed to the desorption of surface water or rearrangements of – OH groups on the oxide surface, and a significant exothermic signal at ~504°C, associated with

surface oxidation processes or late structural reorganization. These transitions are typical of metal oxides with exposed active centres and are in line with the losses observed in TG at similar temperatures (5,32).

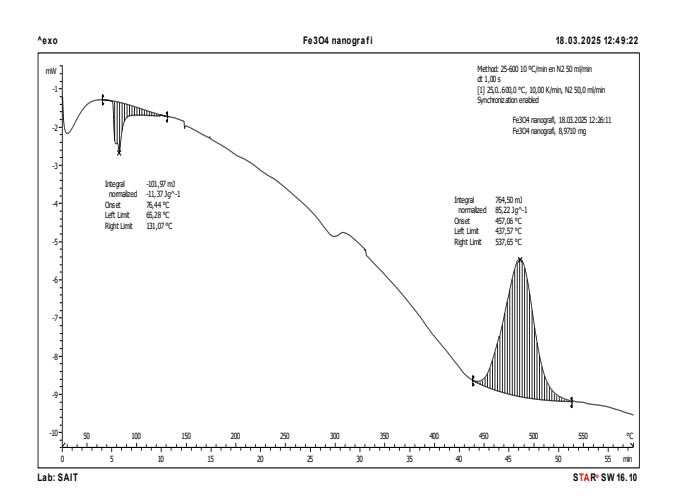


Fig. 18. Heat curve (DSC) of the pure magnetite sample (Fe₃O₄). An endothermic transition is observed around 121°C, attributed to surface water loss or reorganization of –OH groups, and an intense exothermic transition at 504°C, corresponding to oxidation or surface reorganization processes.

For its part, the silver-functionalized sample (Figure 19) also exhibits two thermal events, but shifted to different temperatures: an earlier endothermic transition at \sim 76°C, and an intense exothermic transition at \sim 457°C. The shift to lower temperatures, accompanied by with a larger area under the exothermic curve (resulting in greater energy release), suggests that functionalization with silver facilitates a more efficient and thermally active surface reorganization without compromising the overall stability of the system (18,22). This effect may be due to a catalytic or energy-facilitating action by silver, which promotes the reorganisation of the Fe₃O₄ surface at lower temperatures (17,33).

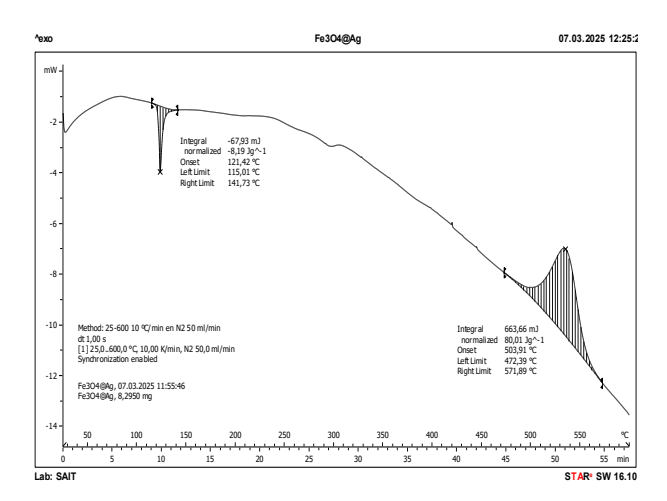


Fig. 19. Heat curve (DSC) of the silver-functionalized magnetite sample (Fe₃O₄@Ag). It shows an earlier endothermic transition (~76°C) and an exothermic signal shifted to a lower temperature (~457°C), with a greater amount of energy released. This thermal features suggest a more active surface reorganization induced by silver.

The results obtained by DSC are in good agreement with the TG observations, which also showed greater thermal stability in the functionalized sample (6). They also correlate with the Raman results, which detected a clear surface reorganization in the presence of silver, and with XPS, which showed silver in a metallic state without the formation of additional oxides(5,7). Together, the DSC data confirm that surface functionalization with silver alters the thermal dynamics of magnetite, promoting earlier and more energetic structural reorganization, with possible positive implications for applied processes involving thermal changes or stability in energy environments (5,22).

For researchers working with thermally responsive nanomaterials, DSC offers valuable insight into surface reactivity and stability, particularly when assessing the impact of surface functionalization with silver on adsorption performance. However, it should be noted that DSC does not provide spatial or chemical resolution. Therefore, its thermal signals must be interpreted in conjunction with structural and spectroscopic techniques to accurately identify the nature of surface changes.

2.7. Brunauer-Emmett-Teller surface area analysis

The BET technique was used to determine the specific surface area of pure magnetite and silver-functionalized magnetite (Fe₃O₄@Ag) samples. This technique, based on nitrogen adsorption at 77 K, allows the quantification of the amount of surface area available for processes such as contaminant adsorption or catalytic interaction. Its application provides crucial insight into the textural accessibility of active sites, especially relevant in adsorption-based removal processes. The measurement of the constant C also provides information on the affinity of the surface towards the adsorbate and the heterogeneity of the system(11,16). The textural characterisation of the samples was carried out using the physical adsorption of nitrogen at 77 K technique, applying the Brunauer–Emmett–Teller (BET) model. The equipment used was a Micromeritics ASAP 2010 system, which allows the specific surface area of the solid to be obtained from the amount of gas adsorbed. The samples were previously degassed to remove impurities that could interfere with the analysis.

The results show a significant increase in surface area after functionalization: pure magnetite has a surface area of 64.41 m²/g, while the functionalized sample reaches 76.47 m²/g, representing an approximate increase of 18.7 %. The observed increase in surface area suggests that silver nanoparticles act not by blocking but by redistributing the surface area, possibly due to a reduction in interparticle aggregation. This result indicates that silver does not seal or block the active surface of the material, but rather increases its accessibility, probably by preventing the agglomeration of nanoparticles and promoting better dispersion (7,10).

The BET equation in its linear form was applied:

$$\frac{P}{V(P_0 \, - \, P)} \, = \, \frac{(C \, - \, 1)}{(V_m \, C)} \, \frac{P}{P_0} + \, \frac{1}{V_m \, C}$$

where P is the equilibrium pressure, P_0 is the saturation pressure, V is the volume of gas adsorbed, V_m is the monolayer capacity, and C is the BET constant related to adsorption energy. These variables were obtained from experimental data and plotted to construct the BET line.

From the regression line, a BET constant $C \approx 220.59$ and monolayer volume $V_m \approx 322.76 \text{ cm}^3/\text{g}$ STP were obtained for Fe₃O₄@Ag. These values were used to calculate the specific surface area, confirming the processed values and indicating a greater exposure of surface sites after functionalization.

Similarly, the C constant in the BET equation increases from 171.96 in Fe₃O₄ to 220.59 in Fe₃O₄@Ag, suggesting a higher interaction energy between the surface and nitrogen molecules after silver functionalization. These results may indicate a more homogeneous surface distribution and enhanced energetic interactions, possibly due to the structuring effect of the silver nanoparticles.

However, it is important to note that BET is limited to providing average values over the surface and does not resolve local heterogeneities or chemical functionality. Additionally, it cannot distinguish between internal and external porosity unless complemented by other methods such BJH (Barrett–Joyner–Halenda), which provides mesopore size distributions, or t-plot analysis, which estimates microporous volume and external surface area.

These results are consistent with observations from other techniques. For example, in laser diffraction, a reduction in average particle size (from 7.98 μm to 6.25 μm) and a lower span value (from 4.03 to 2.24) were detected, indicating a more homogeneous and better dispersed system. Thermal analyses (TG and DSC) revealed more stable profiles and smoother slopes in the functionalized sample, supporting the notion of a more passivated but yet active surface. Finally, in Raman, the disappearance of the typical vibrational modes of hematite suggests a surface structural reorganization, consistent with a rougher or partially amorphous morphology. Although a detailed discussion of the laser diffraction technique will be presented later, its relevance is anticipated in this context. As will be seen, its results reinforce BET observations by highlighting changes in particle size distribution and confirming the improved dispersion and homogenization conferred by silver functionalization.

Taken together, BET analysis contributes a quantitative evaluation of surface availability that complements the structural information from SEM/TEM and the chemical detail from FTIR and XPS. For researchers aiming to assess the suitability of nanomaterials for contaminant capture or catalysis, the BET method provides a foundational parameter but must be integrated with spectroscopic and microscopic techniques for a comprehensive interpretation.

Nonetheless, for researchers evaluating materials for adsorption, BET provides essential and quantitative information on surface accessibility. Its simplicity, reproducibility and interpretative power make it a standard in surface science. When properly combined with structural and spectroscopic techniques, BET helps construct a coherent picture of surface morphology, functionality, and application potential.

2.8. Zeta potential and point of zero charge

Determining the zeta potential as a function of pH is an essential tool for characterizing the surface of colloidal materials, as it allows the ZCP to be identified, i.e. the pH at which the surface of the material has no net charge. This information is crucial in studies of adsorption, colloidal stability and functional material design, since surface electrostatic behaviour directly affects interaction with charged species (5,6,10). The characterisation of particle size and Zeta potential was carried out using a Zetasizer Nano ZS analyser (Malvern Instruments Ltd., United Kingdom), which allows the electrophoretic mobility of particles in suspension to be determined. The method is based on light scattering and the Doppler effect to estimate the migration velocity of particles in an electric field. Zeta potential analysis is used to evaluate the stability of colloidal suspensions and can help to understand the interaction between particles in liquid media.

In this study, this technique was applied to magnetite (Fe₃O₄) nanoparticles and silverfunctionalized magnetite (Fe₃O₄@Ag) nanoparticles, with the aim of evaluating how silver modification alters electrokinetic properties. The starting hypothesis is that the incorporation of silver modifies the surface chemistry, affecting the acid-base behaviour and, therefore, the ability to attract or repel ions under different pH conditions (10,22).

The experimental results shown in Figure 20 reveal notable differences between pure magnetite and its silver-functionalized magnetite. The experimental results show notable differences between the two materials. Pure magnetite has a zero charge point close to pH 7.3, and as the pH increases, its zeta potential becomes increasingly negative, reaching values of approximately -31 mV at pH 10. This behaviour is characteristic of iron oxides, whose surface deprotonates in a basic medium and acquires a negative charge. On the other hand, the silver-functionalized sample shows a shift of the PZC towards more acidic values (\sim pH 6.7) and maintains more positive zeta potentials throughout the measured acid range, suggesting a modification in acidity and surface charge density (10). As a result, the functionalized surface shows a greater affinity for anionic species, reinforcing its potential as a selective adsorbent under environmental conditions (22).

In addition, the slope of the zeta curve vs. pH in the functionalized sample is more pronounced, suggesting greater surface sensitivity to environmental changes, possibly due to new ionization sites generated by silver or electronic redistribution at the solid-liquid interface (6,10).

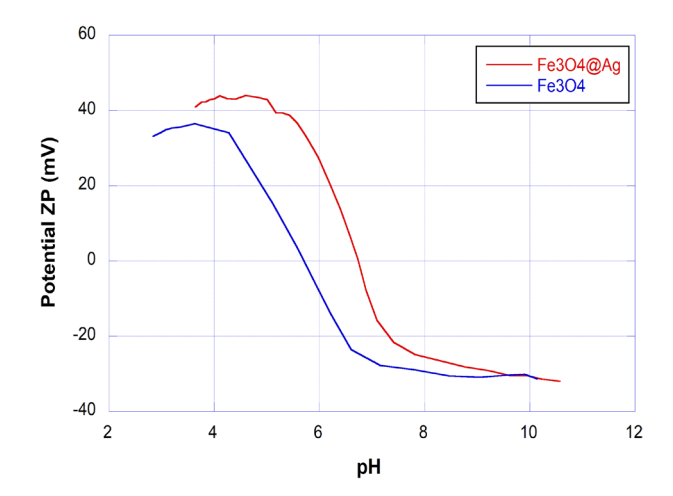


Fig. 20. Zeta potential as a function of pH for Fe₃O₄ and Fe₃O₄@Ag. Functionalization with silver shifts the zero charge point towards more acidic values and increases the positive charge in acidic media, indicating a surface electrostatic modification that favours interaction with anionic contaminants.

Overall, the results obtained demonstrate that the functionalization of magnetite with silver significantly modifies its surface behaviour, shifting the zero charge point towards more acidic values and increasing the positive charge in low pH media. These modifications improve its potential efficiency as an adsorbent of anionic contaminants, as they favour electrostatic attraction under certain pH conditions. This interpretation is consistent with the XPS results, which show electronic reorganization on the surface without the formation of additional oxides, and with Raman, which shows a change in the vibrational modes of Fe–O, suggesting a surface structural alteration consistent with a new charge distribution (5,6,18). Therefore, zeta potential analysis not only allows the surface charge of the material to be characterized but also provides key information for anticipating its functional performance in environmental adsorption processes and technological applications.

Among the main advantages of the PZC determination is its simplicity and its ability to predict electrostatic interactions in adsorption systems. However, it has certain limitations: it does not distinguish between different adsorption mechanisms (e.g., physical vs. chemical adsorption), it is sensitive to ionic strength and to the presence of surface-active groups, and it does not provide molecular-level information. Therefore, its interpretation must be integrated with more specific techniques to develop a comprehensive adsorption model.

In conclusion, the Zero Point of Charge measurement provides critical insight into the surface properties of the adsorbent and its interaction with ionic species such as nitrate. Its role becomes even more relevant when combined with spectroscopic and microscopic methods, which together validate the adsorption mechanism and the effects of surface modification after functionalization. This integrated approach enhances the reliability of the interpretation and optimizes the design of nanomaterials for contaminant removal applications.

2.9. Laser diffraction particle size analysis

The laser diffraction technique allows the particle size distribution in dispersed media to be determined by analyzing the angular intensity of the light scattered by the particles present in the sample. It is a non-destructive, high-resolution technique that provides information on the average volumetric size, the average surface area, the estimated specific surface area and the dispersion index or span, which quantifies the heterogeneity of the system. In this study, this technique was applied to compare the morphometric properties of pure magnetite (Fe₃O₄) with those of silver-functionalized magnetite (Fe₃O₄@Ag), with the aim of evaluating whether the surface modification induced by silver alters the distribution and colloidal stability of the system (10,32). Particle size analysis was performed using a Mastersizer 2000 (Malvern Instruments Ltd.), which determines particle size distribution by measuring the angular dispersion of laser light in a liquid medium. The system operates in a particle size range from 0.02 to 2000 μ m, with different optical configurations

depending on the required measurement interval. The technique is based on Fraunhofer and Mie diffraction models and is particularly useful for characterising colloidal suspensions and functionalised nanoparticles.

The results, as illustrated in Figure 21 and Figure 22, show notable differences between the two samples. In the case of pure magnetite, a mean volume size (D[4,3]) of 7.98 μ m, a mean surface area (D[3,2]) of 2.19 μ m, a specific surface area of 16.71 m²/g, and a span of 4.03 were obtained, indicating a broad and polydisperse distribution, possibly associated with partial aggregation and size heterogeneity. In contrast, the silver-functionalized sample had a mean D[4,3] of 6.25 μ m, a D[3,2] value of 2.06 μ m, a specific surface area of 12.19 m²/g, and a span of 2.24, implying a narrower and more homogeneous distribution. The significant decrease in span reflects an improvement in the dispersion of the system and a lower tendency to agglomeration. Furthermore, the slight reduction in D[3,2] suggests that silver does not cause particle growth but rather stabilizes their original distribution (12,32).

Among its advantages, laser diffraction provides rapid and reproducible analysis across broad size range. However, it assumes particle sphericity, which may bias estimates in anisotropic or aggregated samples. Its data should be complemented with imaging or surface-based techniques for complete characterization. Moreover, this technique can be particularly informative in future analyses aimed at assessing changes in dispersion and particle structure in other functionalized systems, as will be explored in subsequent sections.

From a physical-chemical point of view, this improvement can be interpreted as a surface coating effect induced by silver, which passivates the active sites of magnetite, reducing surface defects, decreasing roughness and limiting attractive interactions between particles. This hypothesis is reinforced by the results obtained in the thermal analysis technique (TG and DSC), where the functionalized sample exhibited less mass loss associated with surface water desorption and earlier thermal reorganization, indicating greater structural stability. Likewise, the decrease in span and the improvement in the uniformity of the system are in line with the zeta potential (PZC) results, where the Fe₃O₄@Ag sample presented a more defined profile, with more positive charges in an acidic medium, suggesting greater colloidal stabilization. Similarly, in images obtained by scanning electron microscopy (SEM), the functionalized particles exhibited better dispersion, without forming dense aggregates. Raman analysis revealed changes in the vibrational modes, particularly the disappearance of signals associated with hematite, indicating a surface reorganization consistent with a more homogeneous structure.

In conclusion, laser diffraction provides quantitative insight into size and dispersion, complementing BET, SEM, TG/DSC and Raman. Its role is pivotal in confirming the impact of silver functionalization on colloidal behaviour, supporting the hypothesis of improved stability and uniformity—which is crucial for adsorption applications in liquid media (10,22).

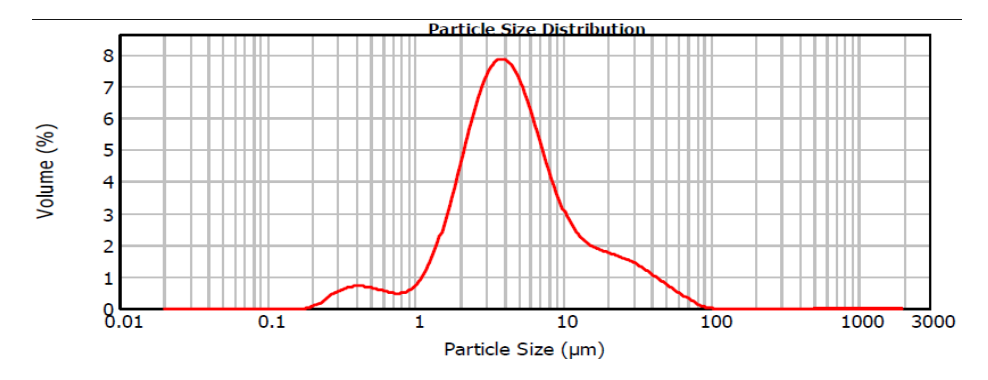


Fig. 21. Particle size distribution – Pure magnetite (Fe_3O_4). The curve obtained by laser diffraction. The distribution reveals a broader profile, with greater size dispersion and a tendency to agglomeration. The mean volumetric size (D[4,3]) is greater, indicating less homogeneity in the system.

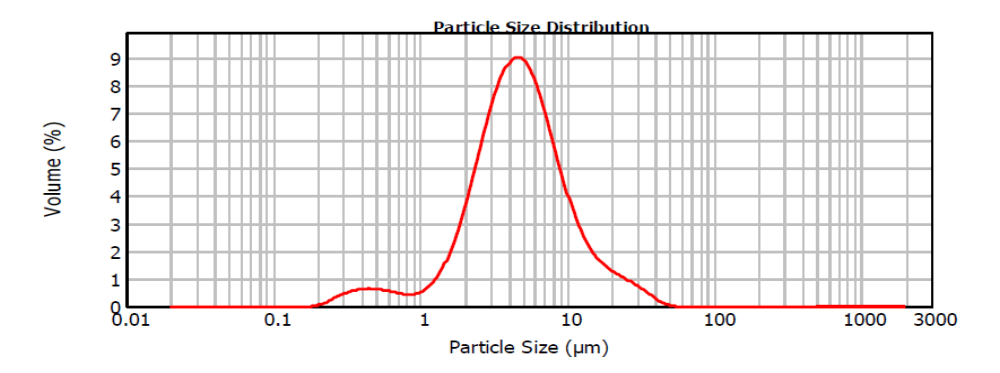


Fig. 22. Particle size distribution — Silver-functionalized magnetite (Fe $_3O_4@Ag$). A narrower and more symmetrical distribution was obtained by laser diffraction, indicating better uniformity and a reduction in the average particle size compared to the non-functionalized sample. Silver functionalization promotes more efficient dispersion and a more stable system.

2.10. X-ray diffraction (XRD)

X-ray diffraction (XRD) is an essential technique for analyzing the crystalline structure of materials, allowing the identification of phases present, the calculation of structural parameters and the detection of possible transformations induced by physical or chemical treatments (5). In this study, samples of pure magnetite (Fe₃O₄) and silver-functionalized magnetite (Fe₃O₄@Ag) were compared to evaluate the structural impact of surface functionalization (18,20,22). Powder X-ray diffraction is performed using BRUKER D8 ADVANCE equipment, designed for the identification of crystalline phases and the structural analysis of solid materials. The system incorporates a vertical theta/theta goniometer with an angular range of 0 to 168° (2θ) and a minimum step of 0.0001°. It is equipped with a 2.2 kW Cu (Kα) ceramic tube, graphite monochromator, NaI(Tl) scintillation detector and rotating sample holder. The X-ray source has a maximum power of 3000 W, with adjustable voltage and current, and features collimation and filtering systems to improve resolution and reduce background noise. The equipment is complemented by DIFFRACPLUS analysis software and ICDD PDF 2, PDF 1 and ICSD databases for automatic phase identification.

The diffractograms obtained (Figure 23) show patterns characteristic of the cubic spinel structure of magnetite, with prominent peaks at angular positions 30.1°, 35.4°, 43.1°, 53.4°, 57.1° and 62.7°, which correspond to the crystallographic planes (220), (311), (400), (422), (511) and (440), respectively, according to the JCPDS: 19-0629 (34,35).

In the case of the Fe₃O₄@Ag sample, additional signals are also observed at 38.1°, 44.3° and 64.4°, corresponding to the (111), (200) and (220) planes of metallic silver. These peaks confirm the presence of silver nanoparticles on the surface and suggest the formation of a secondary phase, without interfering with the original crystal lattice (16,22).

This evidence confirms that silver is incorporated as a segregated phase in the form of metallic nanoparticles on the surface of magnetite, without acting as an internal dopant. This structural behaviour is consistent with the results of Raman spectroscopy, where changes in surface vibration were observed, and with XPS, which confirmed the presence of silver in a metallic state without forming oxides (18,20,22). In turn, the structural stability observed here complements the results of TG and DSC, which showed thermal improvements in the functionalized sample (5,18).

Among its advantages, DRX provides unambiguous identification of the crystalline phases present, as well as a reliable estimate of the size of crystallite size. However, it has limitations such as the inability to detect amorphous phases or distinguish between ultrathin coatings that do not generate significant diffraction.

Overall, the XRD technique confirms that functionalization with silver does not alter the crystalline structure of magnetite, preserving its cubic spinel phase and contributing to greater stability without inducing internal structural transformations (36,37). These findings support the proposed model of weak surface interaction, which will be reinforced with other techniques in the following sections. This biphasic configuration is crucial for applications where it is necessary to

preserve the magnetic properties of magnetite while simultaneously introducing new properties such as conductivity or surface reactivity (20,22).

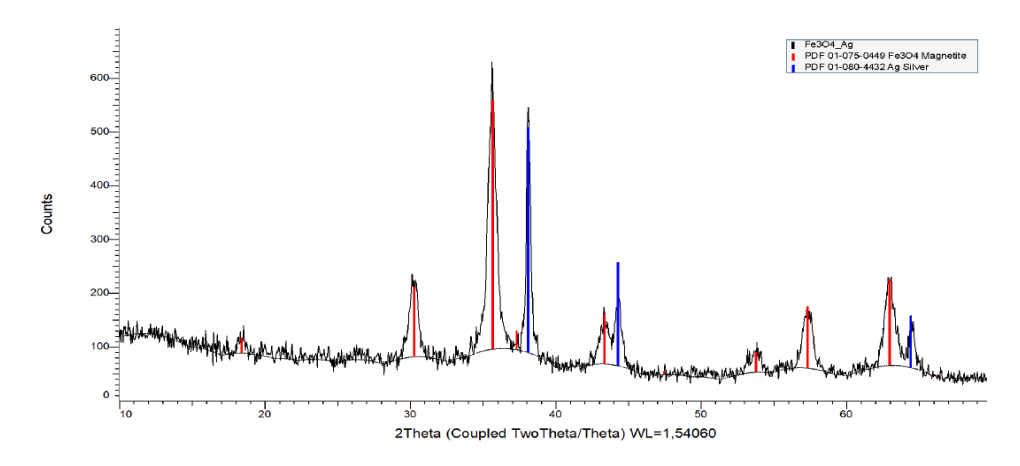


Fig. 23. XRD diffractogram of the Fe₃O₄@Ag sample. The pattern shows the characteristic peaks of magnetite, located at $2\theta \approx 30.1^{\circ}$, 35.4° , 43.1° , 53.4° , 57.1° and 62.7° , confirming the cubic structure of Fe₃O₄. In addition, additional peaks are observed at 38.1° , 44.3° and 64.4° , corresponding to metallic silver, indicating that silver has been incorporated into the system without altering the main crystal structure of magnetite.

3. Magnetometry

Magnetometry is an essential technique for evaluating the magnetic properties of nanomaterials, both in static (DC) and dynamic (AC) regimes. It allows the response of systems to applied magnetic fields and temperature variations to be analyzed, providing key information on parameters such as saturation magnetization (Ms), coercivity (Hc), blocking temperature (TB) and dynamic susceptibility. Magnetic characterisation was performed using a SQUID magnetometer model MPMS XL-7 (Quantum Design), which allows the magnetic moment to be measured as a function of the applied field (up to ± 7 T) and temperature (range between 1.8 K and 400 K). Magnetisation curves versus field (M vs. H) were recorded at 2 K and 300 K, and magnetisation measurements were performed as a function of temperature under an applied field of 50 Oe, using zero-field cooling (ZFC) and field cooling (FC) protocols. The ZFC/FC measurements were performed only at 50 Oe, as the results obtained at higher fields did not show significant differences and were not included in the analysis.

Magnetic characterization was carried out using DC measurements (hysteresis and ZFC–FC curves) and AC measurements (susceptibility as a function of temperature and frequency), comparing pure magnetite with the silver-functionalized sample (Fe₃O₄@Ag).

Figure 24 shows the M vs H magnetization curves at 2 K for both samples. A blocked behaviour is observed at low temperature, with well-defined hysteresis in both cases. The Fe₃O₄ sample has a saturation magnetization of approximately 70 emu/g and a coercive field (Hc) of 325 Oe. The silver-functionalized sample, on the other hand, has a reduced Ms (~62 emu/g), which is attributed to a non-magnetic surface coating by the silver layer. The similarity in Hc (~316 Oe) indicates that functionalization does not significantly alter coercive anisotropy, which is consistent with previous studies (38,39).

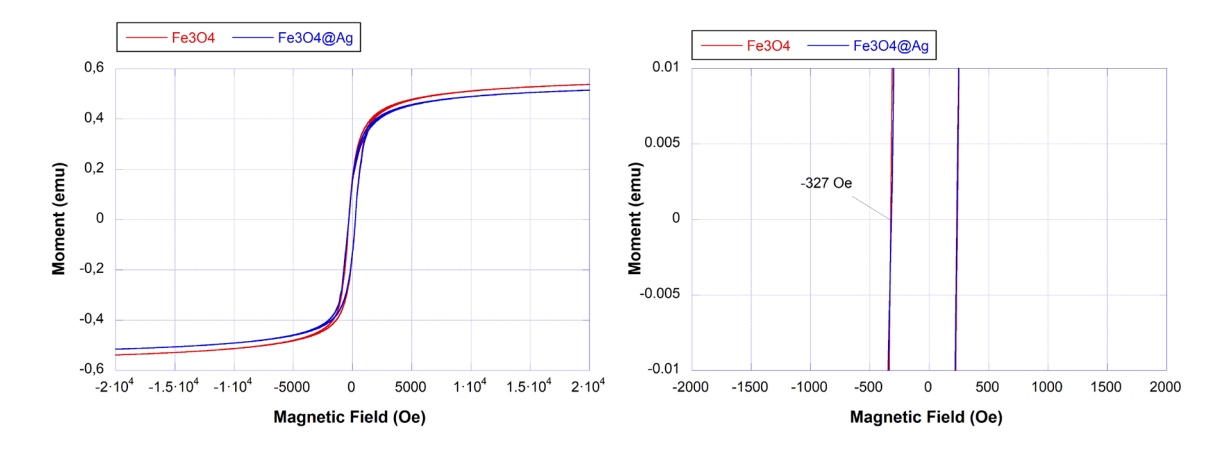


Fig. 24 a) and b). Representative magnetometry curves. a) Hystereses M vs H at 2 K for Fe_3O_4 and Fe_3O_4 (a) Ag. b) Zoomed-in view of the central region showing the coercive field (Hc \approx -327 Oe) and differences near zero field.

The ZFC and FC curves (Figure 25), recorded at an applied field of 50 Oe, show bifurcations characteristic of superparamagnetic systems with size distribution. The blocking temperature (TB) for Fe₃O₄ is around 196 K, while for Fe₃O₄@Ag it drops slightly to ~180 K. This reduction can be attributed to a decrease in effective magnetic anisotropy, a consequence of the interaction between the magnetic surface and the metal layer. In this study, the blocking temperature was determined using the inflection point of the ZFC curve (i.e., the maximum of its derivative dM/dT), rather than the magnetization peak, as this criterion better reflects the transition dynamics in functionalized magnetic systems. The irreversibility temperature (T_{irr}) reaches 300 K in both samples, suggesting a particle size close to the superparamagnetic threshold at room temperature. These observations are consistent with those reported by (39).

On the other hand, AC susceptibility measurements (not shown here) reveal a maximum at approximately 25 K, indicative of a possible spin-glass state in both samples. This behaviour, also observed by (38), could be due to weak interactions between particles or surface frustration effects induced by silver functionalization. The absence of a pronounced maximum around 180 K supports the hypothesis of broad dynamic relaxation, characteristic of systems with size distributions and partially passivated surfaces.

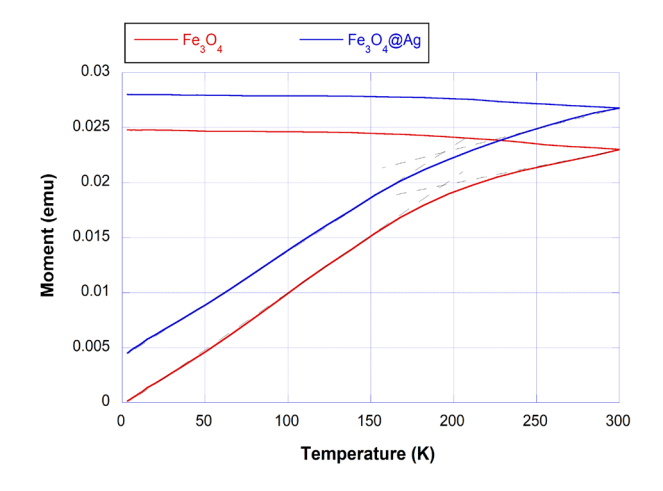


Fig. 25. ZFC and FC curves at 50 Oe. Functionalization with silver slightly decreases the saturation magnetisation and the blocking temperature, with the irreversibility temperature remaining at 300 K.

Magnetic characterization, both DC and AC, provides functional and energy validation of the system studied, confirming and integrating the structural, morphological and surface findings detected by the other techniques.

The results obtained by TEM indicate that silver generates a surface coating—either continuous or partial—on the Fe₃O₄ core without giving rise to new crystalline phases. This morphological arrangement results in a reduction in saturation magnetization (Ms), as the magnetic volume of the core is partially passivated by the metallic coating. On the other hand, XPS analysis revealed that silver is mainly in the metallic state (Ago), with no evidence of strong electronic interaction with iron (Fe 2p). However, physical surface adsorption was observed, which has magnetic consequences, such as a decrease in the blocking temperature (TB) in the ZFC-FC curves, attributed to a modification of the effective anisotropy. The data provided by Raman and XRD confirmed the absence of secondary oxides and oxidized silver species (such as Ag₂O or AgO), with the magnetite core structure remaining intact. This structural stability is supported by the magnetometry results, where the coercivity remains practically constant (~316 Oe in Fe₃O₄@Ag compared to 325 Oe in Fe₃O₄), indicating that the silver coating does not affect the internal magnetic architecture, but only its surface environment. Finally, evidence obtained by FTIR and other surface techniques revealed a slight chemical modification on the surface after functionalization. This change is also reflected in the magnetic response, with a broadening of the dynamic relaxation distribution, as evidenced by the shift of the AC susceptibility maximum towards 25 K. This behaviour is characteristic of spin-glass-type systems, derived from weak interactions and surface inhomogeneities.

Overall, magnetometry is positioned as the integrating technique, translating the structural alterations detected by XRD, the morphological alterations observed by TEM, and the surface interactions revealed by XPS, FTIR, and Raman into magnetic properties. Magnetometry not only validates the preservation of the ferrimagnetic nature of Fe₃O₄ after functionalization but also allows the quantification of the effect of silver on the anisotropy energy, the active magnetic volume and the relaxation dynamics. It thus becomes the essential tool for connecting structural and surface modifications with the functional response of the material, completing the characterization from a physical-magnetic approach.

4. Conclusions

The comprehensive characterization of the Fe₃O₄@Ag system using thirteen structural, surface, thermal and electrokinetic techniques has made it possible to firmly establish the type of interaction between silver and magnetite, as well as its functional implications. The results obtained by XPS, TEM, Raman and FTIR confirm that metallic silver (Ag⁰) is deposited on the surface without integrating into the oxide crystal lattice or forming chemical bonds with iron or oxygen. The absence of silver oxides, shifts in the electronic levels of iron and new vibrational modes supports the hypothesis of a predominantly physical interaction without electronic exchange or the formation of covalent bonds.

At the morphological level, TEM and SEM techniques reveal superficial Ag–Ag metal clusters distributed unevenly on the magnetite, which induce a physical reorganization of the surface. These clusters have metallic bonds between the silver atoms, remaining in a metallic state (Ago), while the interaction with the magnetite surface occurs through Van der Waals forces and London dispersion without the formation of covalent or ionic bonds. This reorganization generates a local electrostatic environment with areas enriched in positive charge, which favours the adsorption of anions such as nitrate. This hypothesis is reinforced by the analysis of the zeta potential (PZC), where a shift of the zero charge point towards more acidic pH values is observed, as well as an increase in positive charge in acidic media.

On the other hand, X-ray diffractograms indicate that the spinel phase of magnetite remains unchanged after functionalization, with no evidence of lattice distortion or silver incorporation into the crystal structure. The appearance of peaks characteristic of metallic silver confirms that it forms an independent surface phase. This result reinforces the exclusively surface nature of the interaction and complements the observations made using spectroscopic and morphological techniques.

In addition, the functionalized system exhibits notable functional improvements, including greater thermal stability (TG, DSC), an increased specific surface area (BET), a reduced tendency to agglomerate (laser diffraction) and a more homogeneous particle size distribution. These combined properties reinforce the material's efficiency as an adsorbent, especially against anionic contaminants in aqueous media. The thermal analysis by DSC reveals shifts in endothermic and exothermic events associated with changes in surface energy and adsorptive capacity, which correlate with the magnetic behaviour observed.

Magnetometry provides a key integrative view of the system's functional performance. The slight decrease in saturation magnetization (Ms) and the reduction in blocking temperature (TB) confirm that silver induces surface passivation without affecting the internal magnetic structure. The magnetic findings thus validate the conclusions drawn from structural and spectroscopic techniques, connecting physical reorganization with functional response. A critical question emerging from these results is to what extent the reduction in Ms is due to a decrease in active magnetic volume caused by the silver coating (surface screening effect) versus a possible alteration in interparticle magnetic interactions. This point remains open to deeper investigation in future studies.

Overall, the results demonstrate that functionalization with silver allows the surface properties of magnetite to be optimized without compromising its internal structure. Silver acts as a highly effective physical and electrostatic modulator, providing a clear functional advantage in environmental applications, particularly in selective adsorption decontamination processes.

References

- [1] Fatahian S, Shahbazi D, Pouladian M, Yousefi MH, Amiri GR, Shahi Z, et al., Digest Journal of Nanomaterials and Biostructures, 2011, 6(3), p.1161;
- [2] Senthil M, Ramesh C., Digest Journal of Nanomaterials and Biostructures, 2012, 7(4), p.1655;
- [3] Jahangirian H, Halim Shah Ismail M, Haron J, Rafiee-Moghaddam R, Shameli K, Hosseini S, et al., Digest Journal of Nanomaterials and Biostructures, 2013, 8(3), p.1263;
- [4] Ghazanfari M, Johar F, Yazdani A., Journal of Ultrafine Grained and Nanostructured Materials [Internet]. 2014 Dec 1 [cited 2025 Apr 17];47(2):97-103.
- [5] Bakr EA, El-Nahass MN, Hamada WM, Fayed TA, RSC Adv [Internet]. 2020 Dec 24 [cited 2025 Apr 17];11(2):781-97; https://doi.org/10.1039/D0RA08230A
- [6] Le TTH, Ngo TT, Nguyen THH, Pham TD, Vu TXH, Tran QV., J Inorg Organomet Polym Mater [Internet]. 2022 Feb 1 [cited 2025 Apr 17];32(2):547-59; https://doi.org/10.1007/s10904-021-02164-1
- [7] Caravaca M, Vicente-Martínez Y, Soto-Meca A, Angulo-González E., Environ Res. 2022 Aug 1;211:113091; https://doi.org/10.1016/j.envres.2022.113091
- [8] Baer DR, Engelhard MH, Johnson GE, Laskin J, Lai J, Mueller K, et al., J Vac Sci Technol A [Internet]. 2013 Sep 1 [cited 2025 Apr 17];31(5); https://doi.org/10.1116/1.4818423
- [9] López-García I, Rengevicova S, Muñoz-Sandoval MJ, Hernández-Córdoba M., Talanta. 2017 Jan 1;162:309-15; https://doi.org/10.1016/j.talanta.2016.10.044
- [10] Vicente-Martínez Y, Caravaca M, Soto-Meca A, Martín-Pereira MÁ, García-Onsurbe MDC, Water 2021, Vol 13, Page 1757; https://doi.org/10.3390/w13131757
- [11] Ebnesajjad S., Applications and Manufacturing. 2011 Jan 1;31-48; https://doi.org/10.1016/B978-1-4377-4461-3.10004-5
- [12] Tahmasebi E, Yamini Y., Anal Chim Acta. 2012 Dec 5;756:13-22; https://doi.org/10.1016/j.aca.2012.10.040
- [13] Lloyd GE., Mineral Mag., 1987 Mar, 51(359):3-19; https://doi.org/10.1180/minmag.1987.051.359.02
- [14] Sánchez E, Torres Deluigi M, Castellano G., Microscopy and Microanalysis, 2012, 18(6):1355-61; https://doi.org/10.1017/S1431927612013566

- [15] Najafpoor A, Norouzian-Ostad R, Alidadi H, Rohani-Bastami T, Davoudi M, Barjasteh-Askari F, et al., J Mol Liq. 2020 Apr 1;303:112640; https://doi.org/10.1016/j.molliq.2020.112640
- [16] Muntean SG, Nistor MA, Ianoş R, Păcurariu C, Căpraru A, Surdu VA., Appl Surf Sci. 2019 Jul 1;481:825-37; https://doi.org/10.1016/j.apsusc.2019.03.161
- [17] Lin Y, Zhi H, Liu S, Chen B, Fu Y, Liu Z., Chemical Papers, 2023 77(4):2115-24; https://doi.org/10.1007/s11696-022-02614-1
- [18] Vicente-Martínez Y, Caravaca M, Soto-Meca A., Environ Chem Lett 2020, 18(3):975-81; https://doi.org/10.1007/s10311-020-00987-x
- [19] Nguyen NT, Nguyen VA., Dig J Nanomater Biostruct 2025 20(2):559-66; https://doi.org/10.15251/DJNB.2025.202.559
- [20] Gong P, Li H, He X, Wang K, Hu J, Tan W, et al., Nanotechnology 2007, 18(28):285604; https://doi.org/10.1088/0957-4484/18/28/285604
- [21] Vicente-Martínez Y, Caravaca M, Soto-Meca A., Chemosphere. 2021, 282:131128; https://doi.org/10.1016/j.chemosphere.2021.131128
- [22] Shan Y, Yang Y, Cao Y, Huang Z., RSC Adv 2015, 5(124):102610-8; https://doi.org/10.1039/C5RA17606A
- [23] Ivanova OS, Lin CR, Edelman IS, Svetlitsky ES, Sokolov AE, Zharkov SM, et al. Appl Surf Sci. 2024 Aug 30;665:160236; https://doi.org/10.1016/j.apsusc.2024.160236
- [24] Jablonski A, Powell CJ., J Electron Spectros Relat Phenomena 2017, 218:1-12; https://doi.org/10.1016/j.elspec.2017.04.008
- [25] Tzomos E, Mikkelä MH, Öhrwall G, Björneholm O, Tchaplyguine M., Surf Sci 2023, 733:122307; https://doi.org/10.1016/j.susc.2023.122307
- [26] Moulder JF., Chastain Jill, King RC., Handbook of x-ray photoelectron spectroscopy: a reference book of standard spectra for identification and interpretation of XPS data. 1995;261.
- [27] Oku M, Hirokawa K., J Electron Spectros Relat Phenomena 1976, 8(5):475-81; https://doi.org/10.1016/0368-2048(76)80034-5
- [28] Gamba O, Noei H, Pavelec J, Bliem R, Schmid M, Diebold U, et al., Journal of Physical Chemistry C 2015, 119(35):20459-65; https://doi.org/10.1021/acs.jpcc.5b05560
- [29] Ferraria AM, Carapeto AP, Botelho Do Rego AM. Vacuum 2012, 86(12):1988-91; https://doi.org/10.1016/j.vacuum.2012.05.031
- [30] Yin H, Jiang L, Liu P, Al-Mamun M, Wang Y, Zhong YL, et al., Nano Res 2018, 11(8):3959-71; https://doi.org/10.1007/s12274-017-1886-7
- [31] Vicente-Martínez Y, Caravaca M, Soto-Meca A, Solana-González R., Scientific Reports 2020, 10(1):1-10.
- [32] Aboulella AM, Wadi VS, Naddeo V, Yousef AF, Banat F, Hasan SW., Chemosphere. 2022, 308:136470; https://doi.org/10.1016/j.chemosphere.2022.136470
- [33] Saeed M, Usman M, Muneer M, Akram N, Ul Haq A, Tariq M, et al., Bull Chem Soc Ethiop 2020, 34(1):123-34; https://doi.org/10.4314/bcse.v34i1.11
- [34] Namikuchi EA, Gaspar RDL, Da Silva DS, Raimundo IM, Mazali IO, Nano Express 2021, 2(2):020022; https://doi.org/10.1088/2632-959X/ac0596
- [35] Chen J, Wang F, Huang K, Liu Y, Liu S., J Alloys Compd 2009, 475(1-2):898-902; https://doi.org/10.1016/j.jallcom.2008.08.064
- [36] Huang QY, Wang SZ, Dong L, Chen C, Zhao XL., Dig J Nanomater Biostruct 19(1):435-42; https://doi.org/10.15251/DJNB.2024.191.435
- [37] Darroudi M, Iftikhar S, Gaigi H, Taj MB, Noor S, Babteen NA, et al., Dig J Nanomater Biostruct 17(2):607-22; https://doi.org/10.15251/DJNB.2022.172.607
- [38] Laha SS, Regmi R, Lawes G., J Phys D Appl Phys 2013, 46(32):325004; https://doi.org/10.1088/0022-3727/46/32/325004

[39] Ounacer M, Essoumhi A, Sajieddine M, Razouk A, Costa BFO, Dubiel SM, et al., J Supercond Nov Magn 2020, 33(10):3249-61; https://doi.org/10.1007/s10948-020-05586-z